

# Synthesis, Characterization and Visible Light Photocatalytic of Fe<sub>3</sub>O<sub>4</sub>/CuO/TiO<sub>2</sub>/Ag Nanocomposites

Malleo Fauzian<sup>1,2</sup>, Ardiansyah Taufik<sup>1,2</sup> and Rosari Saleh<sup>1,2</sup>

<sup>1</sup>Departemen Fisika, Fakultas MIPA-Universitas Indonesia, 16424 Depok, Indonesia

<sup>2</sup>Integrated Laboratory of Energy and Environment, Fakultas MIPA-Universitas Indonesia, 16424 Depok, Indonesia

E-mail: malleo.e604@gmail.com, ardiansyah.taufik@ui.ac.id,  
rosari.saleh@gmail.com

**Abstract.** The sol-gel method was used to synthesize Fe<sub>3</sub>O<sub>4</sub>/CuO/TiO<sub>2</sub>/Ag visible light photocatalyst. X-ray diffraction (XRD) and ultraviolet-visible (UV-Vis) spectroscopy were used to characterize the photocatalyst. From the UV-Vis absorption spectra, we found the surface plasmon resonance (SPR) to be around ~440 nm. The results indicate that the nanocomposites contained a combination of the desired nanocomposites. Their photocatalytic activity was evaluated from the degradation of methylene blue. The influence on the activity of the Fe<sub>3</sub>O<sub>4</sub>/CuO/TiO<sub>2</sub>/Ag nanocomposites, such as weight percentage of Ag, was also studied. Fe<sub>3</sub>O<sub>4</sub>/CuO/TiO<sub>2</sub>/Ag with 25wt% of Ag exhibited the best photocatalytic activity under visible light irradiation. The experiment results showed that the main active species in the photodegradation mechanism in methylene blue is holes. Finally, the nanocomposites exhibited good stability after being reused four times in a cycling process.

## 1. Introduction

With the recent rise in environmental problems, the treatment of various organic pollutants in wastewater is a major issue. Semiconductors have recently been used for degradation of organic pollutants in wastewater. Among all semiconductors, TiO<sub>2</sub> has been widely used in the photodegradation of organic pollutants because of its nontoxicity, low cost, and good photocatalytic activity [1-4]. However, TiO<sub>2</sub> can only be excited under ultraviolet irradiation, resulting in low utilization of solar energy, because of which TiO<sub>2</sub> has a high electron-hole recombination rate. This is a disadvantage in the utilization of the photocatalytic activity of TiO<sub>2</sub> [5-8]. This limitation can be overcome by employing methods such as doping [9], coupling with another semiconductor [10], and deposition of noble metals [11]. Our research group has reported the synthesis and characterization of coupled TiO<sub>2</sub> with another semiconductor, CuO and Fe<sub>3</sub>O<sub>4</sub>, creating Fe<sub>3</sub>O<sub>4</sub>/CuO/TiO<sub>2</sub> nanocomposites with good photocatalytic activity under ultraviolet irradiation. However, the degradation efficiency in the visible light region still requires improvement. Noble metals, such as Au, Ag, and Pt, have often been coupled with TiO<sub>2</sub> nanoparticles to enhance the photocatalytic efficiency under visible light irradiation [12, 13]. The noble metals can promote the interfacial charge transfer process in the composites system and electron traps.

The research aims to study the synthesis and characterization of Fe<sub>3</sub>O<sub>4</sub>/CuO/TiO<sub>2</sub>/Ag nanocomposites and to investigate the effect of incorporating Ag in Fe<sub>3</sub>O<sub>4</sub>/CuO/TiO<sub>2</sub> as a catalyst for degradation of methylene blue under visible light irradiation. The influence of different weight percentages of Ag in Fe<sub>3</sub>O<sub>4</sub>/CuO/TiO<sub>2</sub> on the photocatalytic efficiency was also evaluated. Radical scavengers were employed to provide an insight into the photodegradation mechanism through different active species.



Finally, also investigated the stability of nanocomposites in photocatalytic process, and the catalyst was reused four times in the cycling processes.

## 2. Experimental

In this research, materials were used such as iron (II) sulfate heptahydrate ( $\text{FeSO}_4 \cdot 7\text{H}_2\text{O}$ , 99%), copper sulfate pentahydrate ( $\text{CuSO}_4 \cdot 5\text{H}_2\text{O}$ , 99%), titanium dioxide ( $\text{TiO}_2$ ), silver nitrate ( $\text{AgNO}_3$ ), sodium hydroxide ( $\text{NaOH}$ ), ethanol, and ethylene glycol (EG) purchased from Merck. All chemical reagents (Merck) were of analytical grade and used without further purification.  $\text{Fe}_3\text{O}_4/\text{CuO}/\text{TiO}_2/\text{Ag}$  nanocomposites were prepared using the sol-gel method [14] with further modification. First,  $\text{TiO}_2$  and  $\text{NaOH}$  were mixed with distilled water. Further, the solution was stirred at  $80^\circ\text{C}$  using a magnetic stirrer.  $\text{Fe}_3\text{O}_4$ ,  $\text{CuO}$ , and  $\text{Ag}$  were dispersed into a solution of ethanol and distilled water and added into the suspension at a particular ratio. After 2 h of stirring and heating, the mixed solution was collected, washed, aged, and then dried at  $125^\circ\text{C}$  for 1 h under vacuum. In this experiment, the molar ratio of  $\text{Fe}_3\text{O}_4$ ,  $\text{CuO}$ , and  $\text{TiO}_2$  was 0.5:1:1, and the amount of  $\text{Ag}$  in  $\text{Fe}_3\text{O}_4/\text{CuO}/\text{TiO}_2$  was varied from 5wt% to 25wt% – FCT/Ag 5wt%, FCT/Ag 15wt%, and FCT/Ag 25wt%.

To determine the structure and phase of the samples, X-ray diffraction (XRD) measurements were carried out using a Rigaku Miniflex 600 X-ray diffractometer with monochromatic  $\text{Cu K}\alpha$  radiation, and the optical properties of the samples were studied using UV-Vis spectroscopy (Hitachi UH-5300) in the 200–750 nm range.

The photocatalytic activity was evaluated from the degradation of the organic pollutant, which in this research is methylene blue (MB), in the presence  $\text{Fe}_3\text{O}_4/\text{CuO}/\text{TiO}_2/\text{Ag}$  nanocomposites in an aqueous solution under visible light using a 50 W halogen lamp. In the experiment, 40 mg of  $\text{Fe}_3\text{O}_4/\text{CuO}/\text{TiO}_2/\text{Ag}$  nanocomposites was added to 100 ml of MB with an initial concentration 20 mg/L. Then, the mixture was stirred for 30 min in the dark to establish desorption–adsorption equilibrium between solution and photocatalyst. The lamp was then turned on, and this was considered ‘time zero’ for the reaction. In this research, the photocatalytic reaction proceeded for 2 h, and samples were collected at regular intervals. To examine the stability of the samples, they were reused four times. After testing, the sample was separated with a solution using an external magnet. A decrease in the concentration of the MB solution was measured by a Shimadzu spectrophotometer at the wavelength of 663 nm.

## 3. Results and discussion

X-ray diffraction spectra of  $\text{Fe}_3\text{O}_4/\text{CuO}/\text{TiO}_2/\text{Ag}$  nanocomposites with various weight percentages of  $\text{Ag}$  are plotted in Fig 1a. The diffraction peaks at  $2\theta = 25.24^\circ$  and  $37.8^\circ$ , which are attributed to the (100) and (004) planes, respectively, are the crystal faces of anatase  $\text{TiO}_2$ . Phase cubic spinel  $\text{Fe}_3\text{O}_4$  was detected at ( $2\theta = 30.14^\circ$ ,  $35.49^\circ$ ,  $43.28^\circ$ ,  $53.76^\circ$ ,  $57.20^\circ$ , and  $62.83^\circ$ ) and monoclinic  $\text{CuO}$  at ( $2\theta = 38.81^\circ$  and  $48.7^\circ$ ). After addition of  $\text{Ag}$  25wt%, new peaks were detected at  $2\theta = 37.52^\circ$ ,  $44.61^\circ$ , and  $64.57^\circ$ , which represents the cubic structure of  $\text{Ag}$ . The absence of  $\text{Ag}$  peaks in other nanocomposites is because the amount of  $\text{Ag}$  is too low compared with the other materials. Table 1 presents the crystallite size calculated according to the Scherrer equation [15-16] and the unit cell parameters of all samples. As can be seen, in the sample with 5–15 wt% of  $\text{Ag}$ , the crystallite size of  $\text{Ag}$  is too small to be detected.

The optical properties of the as-prepared samples were determined from the UV–vis absorbance spectra. As shown in Fig 1b,  $\text{Fe}_3\text{O}_4/\text{CuO}/\text{TiO}_2/\text{Ag}$  nanocomposites with various weight percentages of  $\text{Ag}$  have absorption peaks at  $\sim 440$  nm, which display typical surface plasmon resonance (SPR) [17]. However, it indicates the presence of  $\text{Ag}$  in the nanocomposites. Coupling  $\text{Ag}$  with a composite is expected to create a Schottky junction. Schottky junctions mainly facilitate electron–hole separation and promote interfacial electron transfer process. Furthermore, in nanocomposites made of  $\text{Ag}$  and  $\text{TiO}_2$ , given that  $\text{Ag}$  is a plasmonic system, one could expect improved absorption, primarily in the visible region. This phenomenon may be beneficial for photocatalytic activity in the visible region.

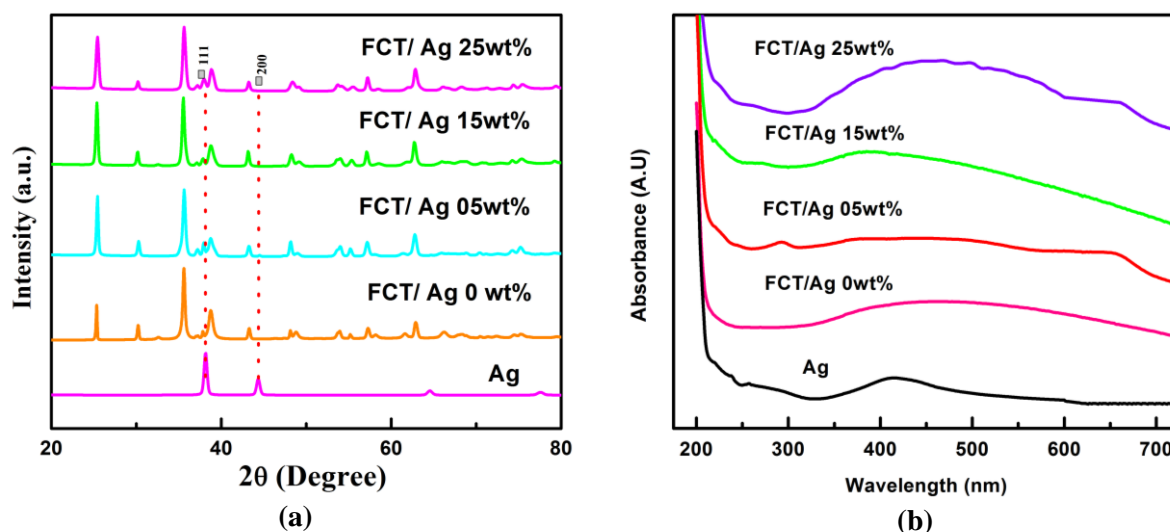


**Figure 1.** (a) XRD spectra and (b) Uv-Vis absorbance spectra of  $\text{Fe}_3\text{O}_4/\text{CuO}/\text{TiO}_2/\text{Ag}$  with various weight percent of Ag.

**Table 1.** Grain Size of  $\text{Fe}_3\text{O}_4/\text{CuO}/\text{TiO}_2/\text{Ag}$  variation weight percent

Samples	Grain Size (nm)			
	$\text{Fe}_3\text{O}_4$	CuO	$\text{TiO}_2$	Ag
$\text{Fe}_3\text{O}_4/\text{CuO}/\text{TiO}_2$	42	15	79	-
$\text{Fe}_3\text{O}_4/\text{CuO}/\text{TiO}_2/\text{Ag}$ 5wt%	40	15	79	-
$\text{Fe}_3\text{O}_4/\text{CuO}/\text{TiO}_2/\text{Ag}$ 15wt%	40	15	78	-
$\text{Fe}_3\text{O}_4/\text{CuO}/\text{TiO}_2/\text{Ag}$ 25wt%	40	14	75	13

Fig 2a shows the photocatalytic activity of  $\text{Fe}_3\text{O}_4/\text{CuO}/\text{TiO}_2/\text{Ag}$  nanocomposites with various weight percentages of Ag based on the degradation of MB under visible irradiation. As can be seen,  $\text{Fe}_3\text{O}_4/\text{CuO}/\text{TiO}_2/\text{Ag}$  nanocomposites with 25 wt% of Ag have the best photocatalytic activity under visible irradiation. It can degrade up to 100% of MB. Incorporation of Ag in the nanocomposites improves the photocatalytic activity owing to SPR in the nanocomposites [18, 19], and with the addition of Ag in the nanocomposites, there is an improvement in the visible light absorption of the nanocomposites.

The influence of dosage catalyst concentration on the degradation of MB using  $\text{Fe}_3\text{O}_4/\text{CuO}/\text{TiO}_2/\text{Ag}$  nanocomposites with 25 wt% of Ag in terms of the photocatalytic activity under visible light irradiation is shown in Fig 2b. The dosage catalyst concentration were varied from 0.1 to 0.4 g/L. With the increase in the dosage catalyst, the degradation of MB was better than that in the case of photocatalytic degradation. A dosage catalyst of 0.4 g/L enhanced the degradation efficiency of MB to 100% within 2 h. This phenomenon may be due to the increase in the surface area of the catalyst to adsorb the MB.

To examine the stability of the catalyst in photocatalytic activity under visible light irradiation, the catalyst was reused four times in a cycling process under the optimum conditions. In this research,  $\text{Fe}_3\text{O}_4/\text{CuO}/\text{TiO}_2/\text{Ag}$  with 25 wt% of Ag could be easily separated from the solution using a permanent magnetic bar. External magnetism is an easy and efficient way to separate the catalyst from the suspension system. The catalyst was reused with the same quantity of fresh MB after each run.

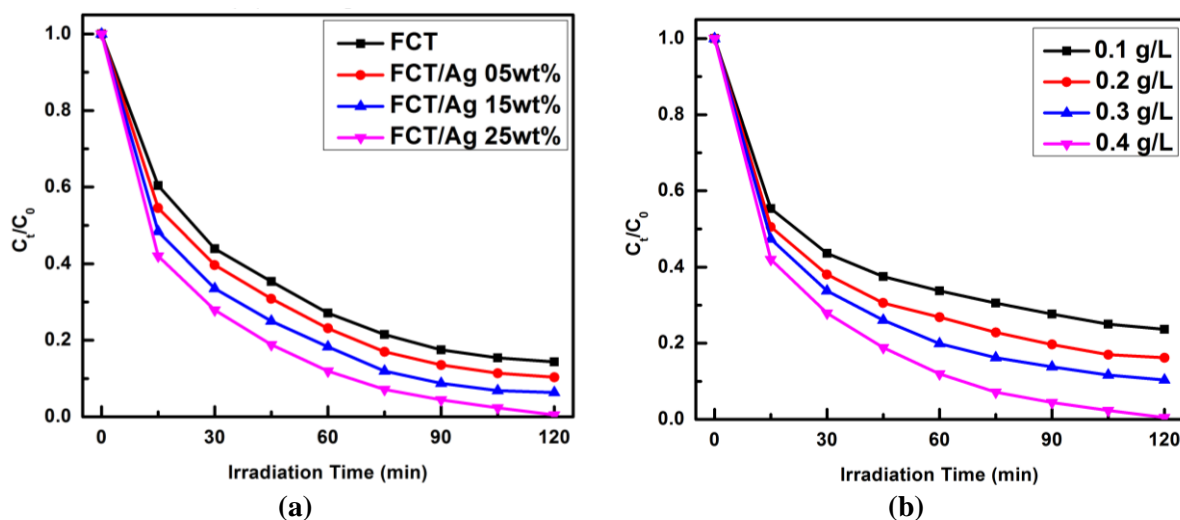


**Figure 2.** (a) Photocatalytic activity and Influence dosage catalyst concentration of Fe<sub>3</sub>O<sub>4</sub>/CuO/TiO<sub>2</sub>/Ag 25wt% to degradation of MB under visible light irradiation.

The results are shown in Fig 3a. As can be seen, after the fourth cycle, degradation of MB slightly declines, only by ~10%. So, it can be concluded that the nanocomposites are stable material after reused fourth time cycling process because contained Fe<sub>3</sub>O<sub>4</sub> in a sample that has a value of magnetization is pretty good, so in the process of separating the sample with a solution becomes easier and the sample is not a lot of wasted.

It is importance to detect the main active oxidative species in the degradation of MB to determine the mechanism of the catalytic activity. Therefore, we control the experiment with the addition of scavengers for electrons, holes, and hydroxyl radicals into the solution under the optimum conditions. Fig 3b shows the degradation of MB in presence of tert-butyl alcohol, diammonium oxalate, and Na<sub>2</sub>S<sub>2</sub>O<sub>8</sub> scavenger for hydroxyl radicals, holes, and electrons, respectively. As can be seen in the figure, after addition of diammonium oxalate in the MB solution, the photodegradation of MB decreased. Thus, the main active species in the experiment is holes.

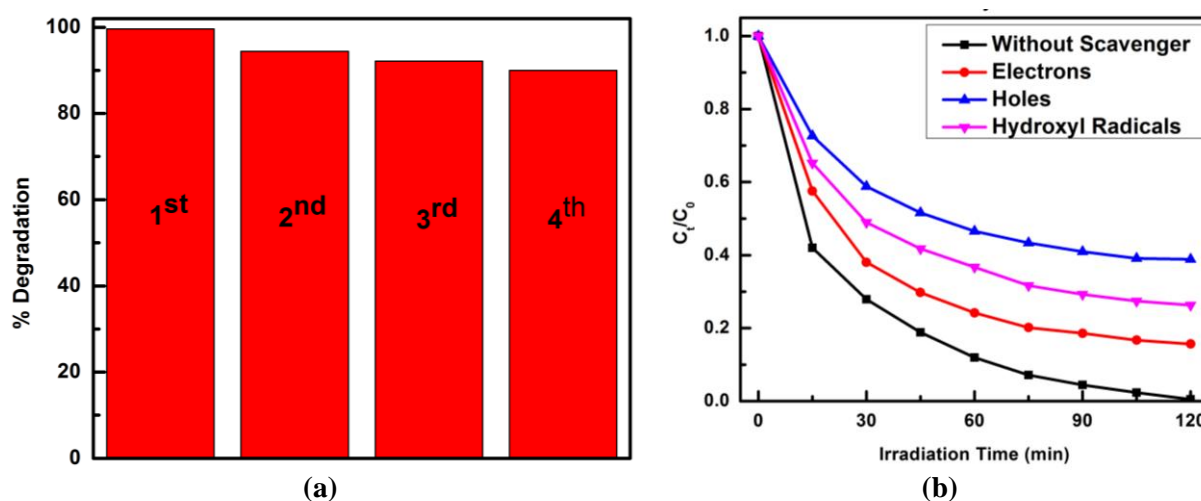


**Figure 3.** (a) Reusability and (b) Effect of different Scavenger of Fe<sub>3</sub>O<sub>4</sub>/CuO/TiO<sub>2</sub>/Ag 25wt% under visible light irradiation.

#### 4. Conclusion

Fe<sub>3</sub>O<sub>4</sub>/CuO/TiO<sub>2</sub>/Ag nanocomposites with various weight percent of Ag were successfully synthesized using sol gel method and active catalyst under visible irradiation for degradation of Methylene Blue (MB). The sample were characterized by using X-ray diffraction (XRD) and Uv-Vis absorbance. It

confirmed that the final Fe<sub>3</sub>O<sub>4</sub>/CuO/TiO<sub>2</sub>/Ag nanocomposites with various weight percent of Ag. Fe<sub>3</sub>O<sub>4</sub>/CuO/TiO<sub>2</sub>/Ag nanocomposites with 25 weight percent of Ag the best photocatalytic activity under visible light to 100% within 2h, this happens due to Surface Plasmons Resonance in nanocomposites and nanocomposites can absorb visible light is much better than the other nanocomposites. Increase dosage catalyst to 0.4 g/L the degradation efficiency of MB because to increase surface area of catalyst to adsorb the MB. Holes is the main active oxidative species in photocatalytic activity on degradation of MB. The catalyst has good stability after reused fourth cycled degradation of MB slightly decline only ~10%.

## References

- [1] M.D. Hernández-Alonso, F. Fresno, S. Suárez, J.M. Coronado, *Energy Environ. Sci.* **2** (2009) pp 1231–1257.
- [2] E. Balaur, J.M. Macak, H. Tsuchiya, P. Schmukiet, *J. Mater. Chem.* **15** (2005) pp 4488–4491.
- [3] D.V. Bavykin, V.N. Parmon, A.A. Lapkin, *J. Mater. Chem.* **14** (2004) pp 3370–3377.
- [4] Z. Liu, D.D. Sun, P. Guo, J.O. Leckie, *Nano. Lett.* **7** (2007) pp 1081–1085.
- [5] B. Ohtani, R.M. Bowman, D.P. Colombo, H. Kominami, H. Noguchi, K. Uosaki, *Chem. Lett.* **27** (1998) pp 579–580.
- [6] S. Ikeda, N. Sugiyama, B. Pal, G. Marci, L. Palmisano, H. Noguchi, *Phys. Chem. Chem. Phys.* **3** (2001) pp 267–273.
- [7] A. Fujishima, X.T. Zhang, D.A. Tryk, *Surf. Sci. Rep.* **63** (2008) pp 515–582
- [8] J. Li, W. H. Ma, Y.P. Huang, X. Tao, J.C. Zhao, Y.M. Xu, *Appl. Catal. B: Environ.* **48** (2004) pp 17-24
- [9] T. Saidani, M. Zaabat, M.S. Aida, B. Boudine, *Superlattices and Microstructures* **88** (2015) pp 315-322
- [10] T. Xu, L. Zhang, H. Cheng, Y. Zhu, *Applied Catalysis B: Environmental* **101** (2011) pp 382-387
- [11] S. Mun Lam, J. Chung Sin, A. ZuhairiAbudllah, A. Rahman Mohamed, *Separataion and Purification Technology* **132** (2014) pp 378-387
- [12] L. Kumaresan, M. Mahalakshmi, M. Palanichamy, V. Synthesis, *Ind. Eng. Chem. Res.* **49** (2010) pp 1480–1485.
- [13] M.R. Mohammadzadeh, M. Bagheri, S. Aghabagheri, Y. Abdi, *Appl. Surf. Sci.* **350** (2015) pp 43–49.
- [14] S. A. Jalaludin, S. A Arifin, R. Saleh, *Material Science Forum* **827** (2015) pp 13-18
- [15] R.Y. Hong, S.Z. Zhang, G.Q. Di, H.Z. Li, Y. Zheng, J. Ding, D, G. Wei, Preparation, *Materials Research Bulletin* **43** (2008) pp 2457-2468.
- [16] A. Hamrouni, H. Lachheb, A. Houas, *Materials Science and Engineering B* **178** (2013) pp 1371- 1379.
- [17] S. S. Patil, M. G. Mali, M. S. Tamboli, D. R. Patil, M. V. Kulkarni, H. Yoon, H. Kim, S. S. Al-Deyab, S. S. Yoon, S. S. Kolekar, B. B. Kale, *Catalysis Today* **260** (2016) pp 126-134
- [18] X. Zhang, L. Wang, C. Liu, Y. Ding, S. Zhang, Y. Zeng, Y. Liu, S. Luo, *Journal of Hazardous Materials* **313** (2016) pp 244-252
- [19] J. Chen, H. Che, K. Huang, C. Liu, W. Shi, *Applied Catalysis B: Enviromental* **192** (2016) pp 134-144